4 Validation of the corrections on an independent database

Using the corrected definition of Sines criterion (equation 10), life predictions in high cycle fatigue are evaluated and compared to experimental results from another experimental database provided by Anes et al. [8;13]. A multiaxial cycle counting method is used based on the Wang-Brown method as presented by Meggiolaro et al. [12].

4.1 Validation database

The experimental database used for validation of the corrected criteria is based on results presented by Anes et al. throughout their work in different publications [8;13;14]. NP tension-torsion fatigue tests on 42CrMo4 samples under a wide range of amplitudes are performed in their work. The number of different loading types as well as the complete information on the 42CrMo4 material are the reasons for the choice of Anes et al. database. Seven loading types are explored (**Fig. 4**). It is worth to notice that only Case1 to Case3 are unicyclic signals in the sense of the Wang-Brown counting method.

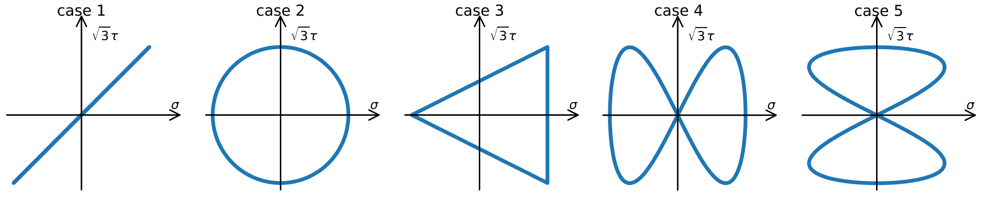

Fig. 4. Validation loadings from V. Anes et al. database [8;13]

4.2 Multiaxial cycle breakdown

Since Case4 to Case5 are not unicyclic, it is necessary to extract cycles using the Wang Brown method as modified by Meggiolaro et al. [12]. This method considers the multiaxial signal in the deviatoric space with J_2 as norm through a geometric algorithm. This allows the definition of multiple half-cycles that can eventually be combined in full cycles. Some remaining half-cycles are to be considered (in the same way the Rainflow counting leaves a residue). When applied to a proportional signal the Wang-Brown method gives the exact same results as the Rainflow counting. This gives good confidence in the NP cycles breakdown. Moreover the Wang-Brown method uses the J_2 norm and in this sense is coherent with both Sines criterion and I_{NP}.

4.3 Finite life prediction

Multiaxial fatigue criterion can be used to predict the number of cycles to failure for each specific loading. This is achieved by writing

$$\begin{cases} \beta_S(N) = A_S N^B, \\ \alpha_S(N) = \alpha_S \end{cases} \tag{11}$$

with $A_S = A_{\tau_{-1}} \frac{\sigma_{-1}}{\tau_{-1}}$, $A_{\tau_{-1}}$ and B being the Basquin parameters of the material. Then, for a given cycle, the lifetime is deduced from equations 10 and 11

$$N_c = \left(\frac{\sigma_{eq_i}}{(1 - a_{corr}I_{NP})A_S}\right)^{1/B} \tag{12}$$

and for a half-cycle :

$$N_h = \frac{1}{2}\left(\frac{\sigma_{eq_i}}{(1 - a_{corr}I_{NP})A_S}\right)^{1/B} \tag{13}$$

The Miner rule is used to determine N_{tot} as the number of full signal repetition before failure

$$N_{tot} = 1\bigg/\left(\sum_{half\ cycles}\frac{1}{N_h} + \sum_{cycles}\frac{1}{N_c}\right) \tag{14}$$

It is worth to notice that each cycle or half cycle for Case4 to Case5 is corrected independently, meaning it is not corrected according the value of I_{NP} of the whole signal but of each corresponding cycle or half cycle. The parameters of the Basquin law as well as the material parameters are extracted from the work of Anes et al. on the 42CrMo4 and Weber [11] (**Table 1**).

Table 1 Material data of the 42CrMo4

Parameter	**σ_{-1} (MPa)**	**τ_{-1} (MPa)**	**σ_0 (MPa)**	**$A_{\tau-1}$ (MPa)**	**B_S=B_C**
Value	398	260	620	864.78	-0.061
Reference	[14]	[14]	[11]	[14]	[14]

4.4 Results

For each loading test the number of cycles to failure is calculated according to equation 12. Preliminary to that a Wang-Brown cycle breakdown is applied for Case4 to Case5. The predicted number of cycles is then compared to the experimental results (**Fig. 5**). The corrected Sines criterion show significantly improved results compared to the non-corrected version.

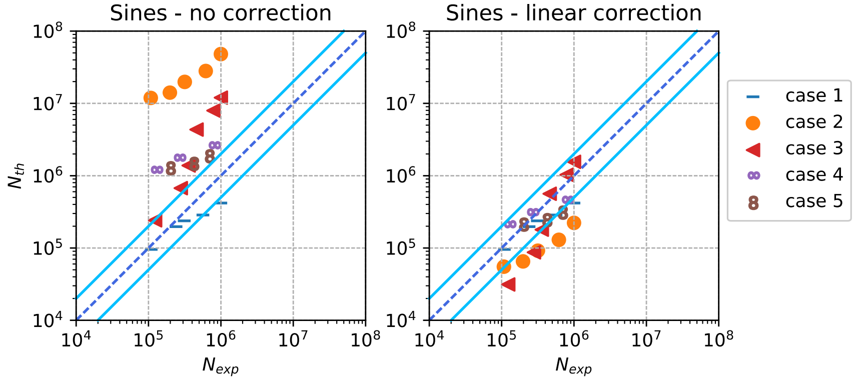

Fig. 5. Results of a linear correction with I_{NP} on Sines criterion

In **Table 2** is detailed the values of I_{NP} of each half-cycle and cycle for Case4 to Case5. ‘Full Signal’ gives the NP degree for the full signal as if it was considered to be one unique cycle. ‘Assembly’ gives a total NP degree according to the following sum

$$I_{NP_{Assembly}} = \sum_i \frac{l_i I_{NP_i}}{\sum_j l_j} \tag{15}$$

with I_{NP_i} the indicator value for one cycle or half-cycle and l_i the length of a cycle/half-cycle according to the J_2 norm. It can be noted that $I_{NP_{signal}} \neq I_{NP_{assembly}}$ meaning the Wang-Brown breakdown affects the NP degree of a signal. This is because the mean value $\underline{\underline{S}}_m$ is used to calculate I_{NP} and this value is not the same for a half-cycle and for the full signal.

Table 2 Mean value of I_{NP} for each loading case

Loading case	Cycle breakdown	I_{NP} Sines	Loading case	Cycle breakdown	I_{NP} Sines
Case5	Full Signal	0.364	**Case6**	Full Signal	0.364
	Cycle 1	0.422		Cycle 1	0.422
	Half-Cycle 1	0.081		Half-Cycle 1	0.081
	Half-Cycle 2	0.165		Half-Cycle 2	0.165
	Assembly	0.326		Assembly	0.324

5 Conclusions

In this study a new invariant based NP indicator is defined and integrated in a full high cycle fatigue lifetime prediction chain based on Sines criterion. Using a complete experimental database this indicator can be used to propose a corrected Sines criterion. Based on another experimental database for multiple NP signals and using the Wang-Brown cycle breakdown method the accuracy of the corrected criterion is demonstrated. The results (**Fig. 5**) show considerable improvements over the original uncorrected approach, both for simple unicyclic signals as well as more complex signals. It should be noted that the Wang-Brown method alters the NP degree of a multiaxial signal as the weighted average of I_{NP} for each cycle is not equal to the value of I_{NP} for the global signal. To achieve an even better correction of the criterion a more sound experimental database could be established. Indeed, as the data collected by Weber [11] are obtained from tests performed between 1945 and 1992, we can assume that the test protocols vary significantly.

References

1. *Fatigue sous sollicitations d'amplitude variable. Méthode Rainflow de comptage des cycles. Principe et utilisation*. (AFNOR, 1993).
2. Wang, C. H. & Brown, M. W. On plastic deformation and fatigue under multiaxial loading. *Nucl. Eng. Des.* **162,** 75–84 (1996).
3. Sines, G. & Ohgi, G. Fatigue Criteria Under Combined Stresses or Strains. *J. Eng. Mater. Technol.* **103,** 82 (1981).
4. Pejkowski, Ł. On the material's sensitivity to non-proportionality of fatigue loading. *Archives of Civil and Mechanical Engineering* **17,** 711–727 (2017).
5. K. Kanazawa, K. J. Miller, M. W. B. Cyclic Deformation of 1% Cr-Mo-V Steel under Out-of-Phase Loads. *Fatigue Fract. Eng. Mater. Struct.* **2,** 217–228 (2017).
6. Fatemi, A. & F. Socie, D. A critical plane approach to multiaxial fatigue damage including out-phase loading. Fatigue Fract. Engng. Mater. Struct. 11, 149-165. *Fatigue Fract. Eng. Mater. Struct.* **11,** 149–165 (1988).
7. Li, B. C., Jiang, C., Han, X. & Li, Y. A new approach of fatigue life prediction for

metallic materials under multiaxial loading. *Int. J. Fatigue* **78,** 1–10 (2015).
8. Anes, V., Reis, L., Li, B. & De Freitas, M. New approach to evaluate non-proportionality in multiaxial loading conditions. *Fatigue Fract. Eng. Mater. Struct.* **37,** 1338–1354 (2014).
9. Vu, Q. H., Halm, D. & Nadot, Y. Multiaxial fatigue criterion for complex loading based on stress invariants. *Int. J. Fatigue* **32,** 1004–1014 (2010).
10. Meggiolaro, M. A. & De Castro, J. T. P. An improved multiaxial rainflow algorithm for non-proportional stress or strain histories - Part I: Enclosing surface methods. *Int. J. Fatigue* **42,** 217–226 (2012).
11. Weber, B. Fatigue multiaxiale des structures industrielles sous chargement quelconque. 243 (1999).
12. Meggiolaro, M. A. & de Castro, J. T. P. An improved multiaxial rainflow algorithm for non-proportional stress or strain histories – Part II: The Modified Wang–Brown method. *Int. J. Fatigue* **42,** 194–206 (2012).
13. Anes, V., Reis, L., Li, B. & De Freitas, M. New cycle counting method for multiaxial fatigue. *Int. J. Fatigue* **67,** 78–94 (2014).
14. Anes, V., Reis, L., Li, B., Fonte, M. & De Freitas, M. New approach for analysis of complex multiaxial loading paths. *Int. J. Fatigue* **62,** 21–33 (2014).